PHILOSOPHICAL TRANSACTIONS OF THE ROYAL SOCIETY A MATHEMATICAL, PHYSICAL & ENGINEERING SCIENCES

The Structure and Energy Balance of Solar Active Regions

Carole Jordan

Phil. Trans. R. Soc. Lond. A 1976 **281**, 391-404
doi: 10.1098/rsta.1976.0037

Phil. Trans. R. Soc. Lond. A. **281**, 391–404 (1976) [391]
Printed in Great Britain

The structure and energy balance of solar active regions

By Carole Jordan
The Appleton Laboratory, Astrophysics Research Division, Culham Laboratory, Abingdon, Oxfordshire

The interpretation of the emission measures calculated from e.u.v. and X-ray line intensities is discussed. A general method for deriving the temperature and density structure and energy balance in either the quiet Sun or active regions is given. In particular simple relations are found between the coronal temperature, the pressure in the chromosphere–corona transition region, P_0, the conductive flux at P_0, the mechanical energy dissipated above P_0 and the radiation losses above P_0. A range of models for quiet and active regions is given. The rate of change of the mechanical energy deposition as a function of height is used to find empirical damping lengths which are compared with those expected from either the conduction damping of sound waves or the viscous damping of Alfvén waves. The wave frequencies and peak amplitude velocities required to satisfy both the empirical and theoretical damping lengths and energy deposition rates are discussed.

1. Introduction

Over the past few years a wide variety of observations of solar active regions has been made in the e.u.v. and X-ray regions of the spectrum. The spectra or spectroheliograms obtained and their interpretation have been the subject of several reviews (e.g. Noyes 1971; Walker 1975; Culhane & Acton 1974; Vaiana, Krieger & Timothy 1973; Jordan 1975).

Most of the models made for the structure of the transition region and corona in quiet and active regions have been derived from the distribution of the emission measure $\int_V N_e^2 \, dV$ which can be calculated from the e.u.v. and X-ray line intensities. It has been usual to combine the observed distribution of the emission measure with conditions imposed by an assumption of constant conductive flux through the transition region, and/or an assumption of hydrostatic equilibrium. In particular Withbroe (1970) found that it was possible to define a quiet Sun model in terms of three parameters, T_c, the coronal temperature, P_0, the pressure at some T_0 in the transition region, and F_c the conductive flux at T_0. In later papers Noyes, Withbroe & Kirshner (1970), Dupree *et al.* (1973) found that the integrated emission from active regions could be accounted for by models defined by the same parameters.

In an earlier paper (Jordan 1975) it was found that by using the observed emission measure, the equation of hydrostatic equilibrium and thermal conduction equation, models could be defined by only two of the above parameters and that the assumption of constant conductive flux was not *a priori* essential. The analytic relations obtained can be applied to individual magnetic flux tubes such as are characteristically observed whenever observations are made with sufficient spatial resolution, and hence the temperature and density structure can be calculated.

In the present paper the above analysis is applied to a range of models and is extended to include the energy balance in the quiet Sun and the range of model flux tubes. The mechanical energy required to be deposited to balance the conductive flux and radiation losses is calculated. The decrease of this energy as a function of height is used to derive empirical damping lengths

which are compared with those expected from, for example, the conduction damping of sound waves and the viscous damping of Alfvén waves. The wave frequencies and peak amplitude velocities that would be implied if either of the above mechanisms was operating are discussed.

2. Analysis of emission measures

The quantity that can be derived from the absolute intensity of a collisionally excited emission line is the emission measure $\int_V N_e^2 \, dV$, where N_e is the electron density and V is the volume of atmosphere over which a given line is formed. The derivation of this quantity is now well known and will not be repeated here. By converting observed fluxes to the equivalent from the whole disk the emission measure can be expressed as $\int_R N_e^2 \, dh$. Assuming a spherically symmetric plane parallel atmosphere the region R can be limited to the temperature range ΔT over which a given line is formed. Thus by observing a wide variety of emission lines formed at different temperatures the distribution of the emission measure as a function of temperature can be found.

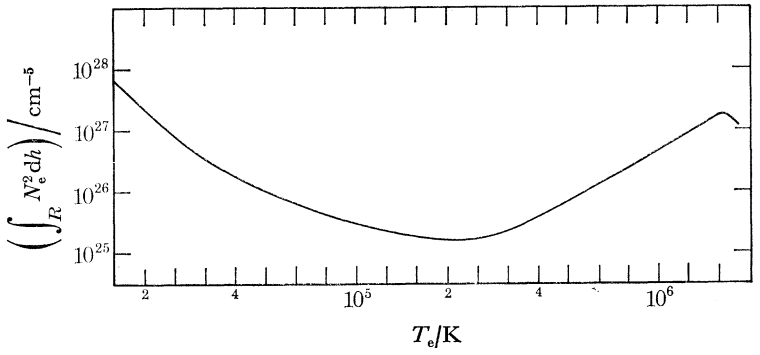

Figure 1. Average emission measure distribution obtained from Burton *et al.* (1971) and Malinovsky & Heroux (1973).

Athay (1966) noticed that in the quiet Sun data he analysed the gradient of the emission measure as a function of temperature had, over the temperature range $10^5\,\mathrm{K} < T_e < 10^6\,\mathrm{K}$ a value close to that expected if there was constant conductive energy flux back from the corona. Figure 1 shows a more recent mean emission measure distribution derived by combining observations by Burton, Jordan, Ridgeley & Wilson (1971) and those by Malinovsky & Heroux (1973). (The intensity corrections recently suggested by these latter authors (private communication) will not substantially change the mean curve.)

The following derivation has been previously discussed (Jordan 1975) but for clarity in later sections it is necessary to repeat it in some detail. The observed distribution of the quiet Sun emission measure shows that between $T_e \approx 10^5\,\mathrm{K}$ and $\approx 10^6\,\mathrm{K}$,

$$\int_{\Delta T} N_e^2 \frac{dh}{dT_e} dT_e = a T_m^b, \tag{1}$$

where a and b are constants, and T_m is an average temperature in the range ΔT, N_e is the electron density. The conductive flux equation is

$$F_c = k T_e^{\frac{5}{2}} dT_e/dh \; 10^{-7}\,\mathrm{J\,cm^{-2}\,s^{-1}}, \tag{2}$$

where the conductive flux is measured downwards.

Defining $P_e = N_e T_e$, and assuming that P_e and dh/dT_e are constant over ΔT, equations (1) and (2) give

$$F_c = \frac{k}{d}\frac{P_e^2}{a} T_e^{-b+\frac{3}{2}}, \tag{3}$$

where $1/d = \Delta \ln T_e$. The temperature interval can be chosen to be the interval over which a certain fraction of each line is formed, e.g. 70 % over $\lg T_m \pm 0.15$. Since this is the fraction usually used in deriving the observed emission measures the numerical constants will correspond to $T_2 = 1.41 T_m$ and $T_1 = 0.70 T_m$, and in the following formulation $T_e = T_m$. However, providing the correct normalization is made to the emission measure distribution smaller intervals can be used until the approximations P_e and dh/dT_e constant over ΔT become satisfactory. The crude assumption for dh/dT becomes important only when variations as a function of T_e are related to variations as a function of height.

From equation (3) it can be seen that conditions for F_c to be constant are $b = \frac{3}{2}$ and P_e is a constant. If a 'constant conductive flux' approximation is used in making models it should be realized that the model may not be in hydrostatic equilibrium. Regarding the precise value of b, Jordan & Wilson (1971) pointed out that the observed emission measure distribution has a gradient which is rather higher than 1.5, and in figure 1 the value is $b = 2.7$. However, the gradient does depend on the relative element abundances used and also on the assumption of a uniform plane parallel atmosphere. Observations of the spatial distribution of the e.u.v. emission, in particular the recent observations from the A.t.m. (Tousey *et al.* 1973; Reeves *et al.* 1974) show that about 85 % of the emission from transition region ions originates from the supergranulation boundaries, which occupy up to about 37 % of the total area. However, by coronal temperatures the emission is essentially uniform. The effect of this variable emitting area on models derived from the emission measure has been previously discussed by Kopp & Kuperus (1968), Kopp (1972), and recently by Gabriel (1975, this volume). To allow for the change in emitting area between 10^5 K and 10^6 K the emission measure at 10^5 K should be raised by the appropriate factor, of about 2.3, which reduces b to 1.2, much closer to the value of 1.5 used by Athay (1966) and assumed by later authors.

A value of $b = 1.5$ will be used throughout the following analysis but the principles are general and other values could be substituted.

The equation of hydrostatic equilibrium can be introduced to give the relation between pressure and temperature as a function of height in either the radial direction or in projection along a given magnetic field line. For temperatures at which hydrogen is fully ionized and for the solar gravity this is

$$\frac{d \lg P_e}{dh} = -\frac{0.86 \times 10^{-4}}{T_e}. \tag{4}$$

Combining equations (1), (2) and (4) gives

$$P_e^2 = P_0^2 - \frac{Da}{(b+1)}[T_e^{\frac{5}{2}} - T_0^{\frac{5}{2}}], \tag{5}$$

where P_0 is the pressure at T_0, at the base of the region over which equation (1) holds. For the quiet Sun $T_0 \approx 2 \times 10^5$ K. $D = 2 \times 0.86 \times 10^{-4} \times d/0.43$. A typical value of '$a$' for the quiet Sun is 3.3×10^{17} (Dupree 1972), and several authors find $P_0 \simeq 6 \times 10^{14}$ cm^{-3} K. From equation (5) it can be seen that $P_e \simeq$ const. (i.e. within 10 % of P_0) for $T_0 < T_e < 7 \times 10^5$ K, and over this region constant conductive flux would be a good assumption.

Now the corona is the region of the solar atmosphere where the temperature is approximately constant. The temperature of this isothermal component, T_c, can be related to the pressure at T_0 and the conductive flux at T_0, $F_c(P_0)$, as follows. At T_c, eventually $P_e \to 0$, hence for $T_c \gg T_0$, from equation (5)

$$T_c^{\frac{5}{2}} = \frac{P_0^2}{a}\frac{1}{D}\frac{5}{2} \tag{6}$$

$$F_c(P_0) = \frac{k}{d}\frac{P_0^2}{a} \tag{7}$$

and

$$F_c(P_0) = k\frac{D}{d}\frac{2}{5}T_c^{\frac{5}{2}}. \tag{8}$$

Withbroe (1970) found also that models of the quiet atmosphere could be described by the three parameters T_c, P_0 and F_c. However, from equations (6) and (7) it can be seen that this reduces to a two-parameter description if one of the parameters is P_0 or a.

The above analysis has been derived from considerations of the quiet solar atmosphere. However, analyses of OSO-IV and OSO-VI data by Noyes *et al.* (1970) and by Dupree *et al.* (1973) have shown that the emission measures found for active regions can be explained in terms of models defined by the same three parameters, P_0, T_c and F_c. This suggests that the above formulation – in particular equation (1) – holds also for active regions. Table 1 shows the conditions derived for the active regions analysed by Noyes *et al.* and Dupree *et al.* and the values expected treating T_c and a as known and using equations (6) and (7) to derive P_0 and $F_c(P_0)$. The parameters a, P_0 and F_c are expressed in terms of their values in the quiet Sun. It can be seen that the agreement between the two methods is reasonable, considering that the spatial resolution of the observations was not high and only average conditions are represented. Equations (2), (3) and (5) can now be used to calculate the variation of F_c, $\mathrm{d}h/\mathrm{d}T_e$ and P_e with T_e for models specified by P_0 and a.

TABLE 1. CORONAL TEMPERATURES AND CONDUCTIVE FLUXES DERIVED FROM BEST FIT TO OBSERVATIONS AND FROM ANALYTICAL EXPRESSIONS

	$\frac{a_A}{a_Q}$	$\frac{P_0(A)}{P_0(Q)}$	$\frac{F_c(A)}{F_c(Q)}$	$\frac{T_c(A)}{K}$	$\frac{T_c(Q)}{K}$
Noyes *et al.* (1970)	5	5	5	2.5×10^6	2.0×10^6
present paper	4†	5†	5‡	2.9×10^6‡	1.5×10^6†
Dupree *et al.* (1972)	8	7	12	3.2×10^6	2.0×10^6
present paper	8†	7†	6‡	3.1×10^6‡	1.5×10^6†

† Input parameters. ‡ Derived parameters.

Although the variations as a function of height can be found by numerical procedures an analytic form can be given for the height, h, above that at T_0, h_0, for $T_e \leqslant 0.9T_c$. This is, for $T_0 \ll T_c$,

$$\int_{h_0}^{h_\theta} \mathrm{d}h = \frac{5}{2}\frac{d}{D}T_c\int_{\theta_0}^{\theta}\frac{\theta^{\frac{5}{2}}}{1-\theta^{\frac{5}{2}}}\,\mathrm{d}\theta. \tag{9}$$

The general integral can be plotted and hence $(h-h_0)$ is simple to calculate as a function of $\theta = T_e/T_c$ (where $P_e^2 \simeq P_0^2$ equation (9) reduces simply to $(h-h_0)/T_e = 5d\theta^{\frac{5}{2}}/7D$).

The active region emission can be considered as originating from a set of magnetically controlled flux tubes, each with its own P_0 and T_c, with equations (1), (2) and (4) holding for each

flux tube. The above formulation assumes that $b = \frac{3}{2}$ takes into account any increase in the cross-section area of the flux tube with height. The equation of conductive flux must be modified by a $\cos\psi$ term, where ψ is the angle between the vertical and the field direction. For flux tubes of sufficient height to develop an 'isothermal' regime this correction is negligible. For flux tubes where the maximum observed temperature is lower than T_c the correction is significant only at $T_e \gtrsim 0.8T_{max}$.

3. Energy balance

The general equation for the energy balance over each region R of the atmosphere can be written as

$$\Delta F_m = \int_R R_{diss}\,dh = \int_R R_{rad}\,dh - \Delta F_c, \tag{10}$$

where $\Delta F_m = \int_R R_{diss}\,dh$ is the mechanical energy deposited by some damping process, $\int_R R_{rad}\,dh$ is the energy lost by radiation and $\Delta F_c = F_c(T_2) - F_c(T_1)$ is the energy input from thermal conduction, with $T_2 > T_1$. Since the 'solar wind' loss is small for the quiet corona and is negligible for closed flux tubes no term for such a loss will be included.

McWhirter, Thonemann & Wilson (1975) have recently recalculated the radiative power loss P_{rad} as a function of T_e. Over the temperature range $10^5\,K \leqslant T_e \leqslant 2\times10^7\,K$ their results can be approximated by

$$P_{rad} = 6.0\times10^{-17}\,T_e^{-1}\,10^{-7}\,J\,cm^{-3}\,s^{-1}. \tag{11}$$

The radiation loss per unit volume is, for solar abundances and hydrogen fully ionized,

$$R_{rad} = 0.80N_e^2\,P_{rad}\,10^{-7}\,J\,cm^{-3}\,s^{-1}. \tag{12}$$

In order to calculate $\int_R R_{rad}\,dh$, ΔF_c and ΔF_m the relation for dh/dT found from equations (2) and (3), i.e. $dh/dT = adT_e^{\frac{5}{2}}/P_e^2$, is used. This was derived by using P_e and dh/dT constant over R but can be used to give mean values at any T_e. Hence through substitution in equation (10)

$$\Delta F_m = \int_R R_{diss}\,dh = 4.8\times10^{-17}ad\int_{\Delta T} T^{-\frac{1}{2}}\,dT - \frac{kD}{d}\,\tfrac{2}{5}[T_1^{\frac{5}{2}} - T_2^{\frac{5}{2}}]\,10^{-7}\,J\,cm^{-2}\,s^{-1}. \tag{13}$$

Substituting $d = 1.4$ (for an interval corresponding to $\lg T_m \pm 0.15$), $D = 5.6\times10^{-4}$, $k = 1.0\times10^{-6}$, and $T_2 = 1.4T_m$, $T_1 = 0.70T_m$ as before, gives

$$\Delta F_m = \int_R R_{diss}\,dh = 5.1\times10^{-17}aT_e^{\frac{1}{2}} + 3.1\times10^{-10}T_e^{\frac{5}{2}}\,10^{-7}\,J\,cm^{-2}\,s^{-1}. \tag{14}$$

Note that if $b = \frac{3}{2}$ then over the temperature range considered the conductive term always represents a loss, i.e. more energy is conducted out of the layer than is conducted in and hence dissipation must occur to balance this and the radiation losses. This is not necessarily the situation for $b \neq \frac{3}{2}$ (Kopp 1972, reached a similar conclusion.) Equation (14) can now be used to evaluate the relative importance of the radiation losses and conduction losses. It can be seen that whereas the conduction loss depends only on T_e the radiation loss also depends on a, and hence equation (1) does not imply that the energy balance is the same for all flux tubes but allows a full range of conditions from the conduction dominated situation to the radiation dominated situation. For the quiet Sun $a = 3.3\times10^{17}$ and in equation (14) the conduction term dominates for $T_e > 6\times10^5\,K$. Thus dissipation occurs not only in the corona to balance conduction but also to a smaller extent in the transition region to balance radiation and conduction.

PHILOSOPHICAL TRANSACTIONS OF THE ROYAL SOCIETY A MATHEMATICAL, PHYSICAL & ENGINEERING SCIENCES

Now the total energy deposited above T_0, i.e. $F_m(P_0)$, can be related to the total radiation loss above T_0 and the conductive flux at T_0. Summation over the whole atmosphere above T_0 gives

$$F_m(P_0) = 1.46 \times 10^{-16} a(T_c^{\frac{1}{2}} - T_0^{\frac{1}{2}}) + 1.6 \times 10^{-10}(T_c^{\frac{5}{2}} - T_0^{\frac{5}{2}}) \quad (15)$$

or

$$F_m(P_0) = 1.46 \times 10^{-16} a(T_c^{\frac{1}{2}} - T_0^{\frac{1}{2}}) + F_c(P_0).$$

Thus not only can $F_c(P_0)$ be simply related to P_0, a and T_c, but also $F_m(P_0)$ can be related to the same parameters. Thus if two of the three parameters P_0, a, T_c, including either P_0 or a, are known then $F_c(P_0)$, $F_m(P_0)$ and the total radiation loss from the plasma at $T_e > T_0$ can be calculated. The above analysis differs from earlier ones by Shmeleva & Syrovatskii (1973) and Moore & Fung (1972) in that the dissipated energy is deduced from the observed emission measure rather than it being assumed that the energy is deposited only at a great height in the atmosphere.

4. Models based on observed conditions

The expressions for the physical conditions in the quiet corona or in flux tubes have been derived using the equations of hydrostatic equilibrium, conductive flux, energy balance and the observed emission measure distribution. In the present section the models calculated from the analytical relationships will be compared with other observed properties of active regions.

The general picture of an active region that has been developed from a wide variety of observations can be summarized as follows. At photospheric levels active regions are characterized by the concentration of magnetic flux, and usually by the presence of sunspots. In the chromosphere, lines such as those of Ca II are enhanced over the whole active region or plage area. This enhancement continues for lines formed at higher temperatures in the transition region and corona (Noyes 1971), and spatially resolved observations (Krieger, Vaiana & Van Speybroeck 1971), and the recent A.t.m. observations have shown that extensive systems of loop-shaped structures, presumably magnetically controlled flux tubes, are associated with the active regions.

Analyses of absolute intensities, particularly in active regions on the limb, have shown that in general the central parts of active regions, at low heights, are hotter and denser than the more extensive surrounding material. Observations with sufficient spatial resolution show that the hot denser central regions are associated with low lying loop structures and the cooler less dense regions with more extensive loops (see, for example, Boardman & Billings 1969; Mason 1975; Gabriel & Jordan 1975; Vaiana *et al.* 1973). One of the characteristic aspects of the loops is that they appear to be isothermal over a large range of their height – observations in emission lines formed at different temperatures reveal distinctly different features. Pneuman (1972) has pointed out that many loop structures will be essentially isothermal due to the high thermal conductivity and has discussed the energy balance in large loops which have a regime where the temperature has passed beyond a maximum value.

By using the analytical relations in the preceding sections, it can be seen that the development of an extensive isothermal component depends on the values of P_0 and a for a given flux tube. P_0 and a determine T_c the maximum temperature which can be reached. However, to reach T_c the height of the flux tube must be greater than the height to $\theta = 0.90$ as given by equation (9). An extensive isothermal regime will only develop when the height of the loop becomes larger than the minimum needed for T_c to be reached. Conversely if the maximum temperature in a loop of known height can be determined then T_c can also be calculated. If P_0 is known then the remaining parameters, a, $F_c(P_0)$ and $F_m(P_0)$ can also be found.

PHILOSOPHICAL TRANSACTIONS OF THE ROYAL SOCIETY A MATHEMATICAL, PHYSICAL & ENGINEERING SCIENCES

TABLE 2. EXAMPLE MODEL PARAMETERS

model	a / $\mathrm{cm^{-5}\,K^{-\frac{3}{2}}}$	P_0 / $\mathrm{cm^{-3}\,K}$	T_o / 10^5 K	T_c / K	$F_c(P_0)$ / $\mathrm{J\,cm^{-2}\,s^{-1}}$	$F_m(P_0)$ / $\mathrm{J\,cm^{-2}\,s^{-1}}$	$\int R_{rad}\,dh$ / $\mathrm{J\,cm^{-2}\,s^{-1}}$	h observed (for loops) / 10^4 km
(1) quiet Sun	3.3×10^{17}	5.6×10^{14}	2	1.78×10^6	6.8×10^{-2}	7.2×10^{-2}	4.3×10^{-3}	—
(2) active region (1970 eclipse data)	2.2×10^{19}	2.0×10^{15}	2	9.3×10^5	1.3×10^{-2}	1.8×10	1.7×10^{-1}	15
(3) active region (1970 eclipse data)	1.5×10^{20}	7.3×10^{15}	2	1.2×10^6	2.5×10^{-2}	1.5	1.4	8.0
(4) active region (1970 eclipse data)	1.0×10^{21}	2.9×10^{16}	2	1.7×10^6	6.0×10^{-2}	1.2×10	1.2×10	5.0
(5) active region (1970 eclipse data)	1.1×10^{20}	1.6×10^{16}	2	2.5×10^6 2.0×10^6†	1.6×10^{-1}	1.8	1.6	3.0
(6) active region (assumed parameters)	2.6×10^{21}	6.0×10^{17}	2	1.3×10^7 6.0×10^6†	9.7	9.6×10	8.6×10	1.5
(7) active region (assumed parameters)	4.0×10^{20}	2.0×10^{18}	2	7.1×10^7 $2{\cdot}0\times10^7$†	6.8×10^2	7.0×10^2	2.5×10	1.5

† T_{max} observed.

TABLE 3. MODELS OF QUIET AND ACTIVE REGIONS

model 1. Quiet Sun $T_c = 1.78\times10^6$ K

lg T_e / K	P_e / 10^{14} $\mathrm{cm^{-3}\,K}$	dT/dh / $\mathrm{K\,cm^{-1}}$	10^2F_c	$10^4\int R_{rad}\,dh$	$-\Delta F_c$ / $\mathrm{J\,cm^{-2}\,s^{-1}}$	ΔF_m	10^2F_m	$\simeq (h-h_0)$ / km
5.3	5.60	3.8×10^{-2}	6.8				7.2	1.4×10
5.4	5.59	2.2×10^{-2}	6.8	2.7	2.1×10^{-4}	4.8×10^{-4}	7.2	3.1×10
5.5	5.57	1.2×10^{-2}	6.7	3.0	4.3×10^{-4}	7.3×10^{-4}	7.1	7.7×10
5.6	5.54	6.6×10^{-3}	6.6	3.3	6.9×10^{-4}	1.0×10^{-3}	7.0	1.7×10^2
5.7	5.49	3.7×10^{-3}	6.5	3.8	1.2×10^{-3}	1.6×10^{-3}	6.8	4.0×10^2
5.8	5.40	2.0×10^{-3}	6.3	4.2	2.2×10^{-3}	2.6×10^{-3}	6.6	8.9×10^2
5.9	5.23	1.0×10^{-3}	5.9	4.7	4.1×10^{-3}	4.6×10^{-3}	6.1	2.3×10^3
6.0	4.91	5.2×10^{-4}	5.2	5.3	6.8×10^{-3}	7.4×10^{-3}	5.5	4.8×10^3
6.1	4.28	2.2×10^{-4}	4.0	5.9	1.2×10^{-2}	1.3×10^{-2}	4.0	1.3×10^4
6.2	2.85	5.6×10^{-5}	1.8	6.7	2.2×10^{-2}	2.2×10^{-2}	1.8	4.2×10^4
6.25	$\to 0$	$\to 0$	$\to 0$	3.6	1.8×10^{-2}	1.8×10^{-2}	$\to 0$	

model 5. Active region, $T_{max} = 2\times10^6$ K

lg T_e / K	P_e / 10^{16} $\mathrm{cm^{-3}\,K}$	dT/dh / $\mathrm{K\,cm^{-1}}$	$10F_c$	$10\int R_{rad}\,dh$	$-\Delta F_c$ / $\mathrm{J\,cm^{-2}\,s^{-1}}$	$10\Delta F_m$	F_m	$\simeq h-h_0$ / km
5.3	1.58	9.0×10^{-2}	1.6				1.8	6.3
5.4	1.58	5.2×10^{-2}	1.6	0.88	2.1×10^{-4}	0.88	1.7	1.4×10
5.5	1.57	2.8×10^{-2}	1.6	0.99	4.3×10^{-4}	1.0	1.6	3.2×10
5.6	1.57	1.6×10^{-2}	1.6	1.1	6.9×10^{-4}	1.1	1.5	7.1×10
5.7	1.56	9.0×10^{-3}	1.6	1.2	1.2×10^{-3}	1.3	1.4	1.6×10^2
5.8	1.55	5.0×10^{-3}	1.6	1.4	2.2×10^{-3}	1.4	1.2	3.6×10^2
5.9	1.53	2.7×10^{-3}	1.5	1.6	4.1×10^{-3}	1.6	1.1	8.8×10^2
6.0	1.50	1.4×10^{-3}	1.5	1.8	6.8×10^{-3}	1.8	0.91	1.9×10^3
6.1	1.43	7.5×10^{-4}	1.3	2.0	1.4×10^{-2}	2.1	0.70	4.5×10^3
6.2†	1.31	3.6×10^{-4}	1.0	2.3	2.6×10^{-2}	2.6	0.44	1.1×10^4
6.3†	1.05	1.3×10^{-4}	$\to 0$	3.4	1.0×10^{-1}	4.4	$\to 0$	3.0×10^4

† Corrected for curvature.

PHILOSOPHICAL TRANSACTIONS OF THE ROYAL SOCIETY A MATHEMATICAL, PHYSICAL & ENGINEERING SCIENCES

Table 2 gives the values of $F_m(P_0)$, $F_c(P_0)$ and $\int R_{rad}\,dh$ which result from a range of density and temperature values. The energies required range from *ca.* 0.07 J cm^{-2} s^{-1} for the quiet Sun to *ca.* 2 J cm^{-2} s^{-1} for the hottest 'observed' loop. The models based on assumed parameters require energies comparable with those normally associated with solar flares. Five models have been made to illustrate the range of conditions which result as a function of P_0 and T_c. One is for quiet Sun conditions, three are for values of P_0 and T_c derived from the analysis by Gabriel & Jordan (1975) of the 1970 total eclipse data, the fifth is based on assumed values of P_0 and T_c to illustrate an even higher temperature situation. Table 3 gives the parameters which specify models 1 and 5.

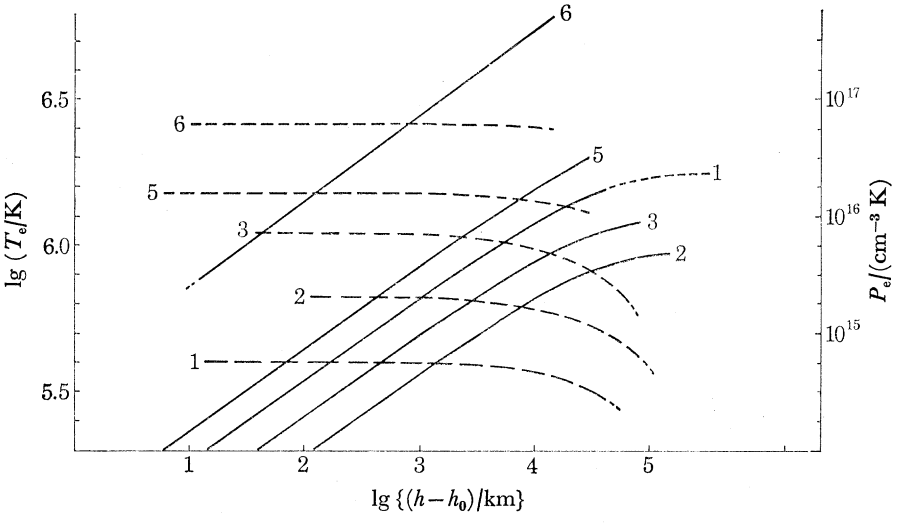

FIGURE 2. The variation of temperature and pressure with height for five models given in table 2; 1 is for the quiet Sun; 2, 3 and 5 are for active region loops; 6 is for a hypothetical hot loop. The temperature curves are given as full lines, the pressure curves as dashed lines.

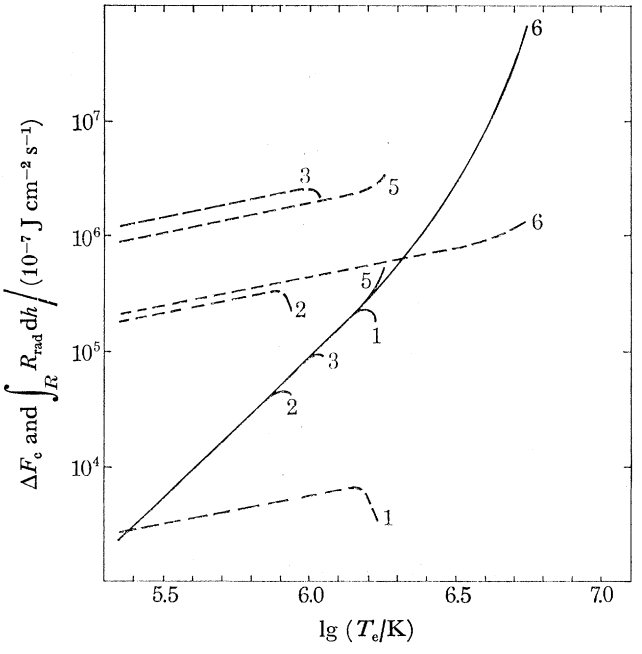

FIGURE 3. The variation of ΔF_c and $\int R_{rad}\,dh$ as a function of temperature for five of the models given in table 2. The curves for ΔF_c are given as full lines and the radiative loss curves as dashed lines.

Figures 2, 3 and 4 show the distributions which result for the variation of density, temperature, conductive flux, radiative loss and mechanical energy deposition, including the further models, 2, 3 and 6. It can be seen that in the active region loops the deposition of energy is more uniform as a function of temperature, and that the overall energy balance is primarily between the radiative losses and the energy deposited. In the hypothetical loops the relative importance of radiation and conduction depends, of course, on the assumed value of P_0.

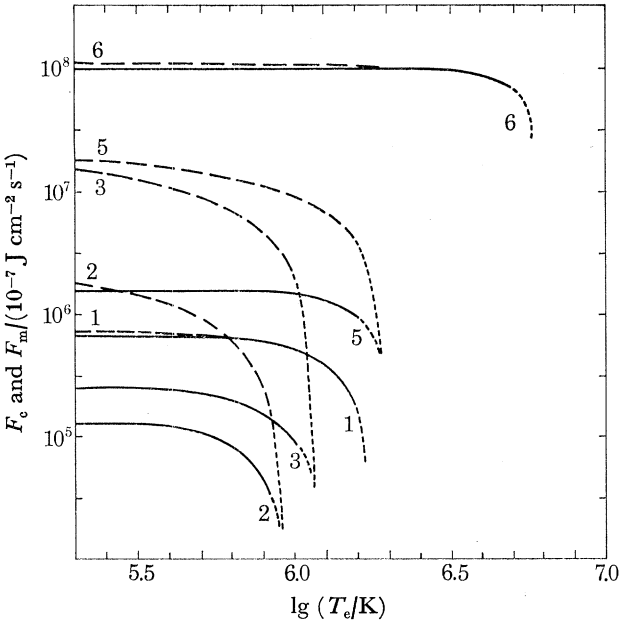

FIGURE 4. The variation of F_m and F_c as a function of temperature for five of the models given in table 2. F_c is plotted as a full line and F_m as a dashed line.

5. THE MECHANICAL ENERGY DEPOSITION

In § 3 an analytical relation was given for the dependence of ΔF_m on a and T_e. This is the dependence derived from the observed emission measures and it is of interest to see how well it can be matched by the dissipation by, for example, damping of (*a*) sound waves, and (*b*) Alfvén waves. The energy carried by a wave is

$$E = \tfrac{1}{2}\rho V^2, \tag{16}$$

where V is the peak wave amplitude velocity and ρ is the density. The energy flux propagated is then

$$\phi = EV_p, \tag{17}$$

where V_p is the wave propagation velocity.

If ϕ is related to observed mechanical motions for which V_m is the r.m.s. velocity then, because of equipartition between the kinetic and potential components,

$$V_m^2 \simeq \tfrac{1}{2}V^2.$$

For sound waves

$$V_p = V_s = (\gamma P/\rho)^{\frac{1}{2}}.$$

For adiabatic sound waves $\gamma = \frac{5}{3}$ and for the solar atmosphere

$$V_s = 1.5 \times 10^4 T_e^{\frac{1}{2}} \text{ cm s}^{-1}. \tag{18}$$

For Alfvén waves $$V_{\rm p} = V_{\rm A} = B_0/(4\pi\rho)^{\frac{1}{2}},$$

where B_0 is the magnetic field strength in gauss (10^{-4} T). Hence

$$V_{\rm A} = 2.0\times 10^{11} B_0 P_{\rm e}^{-\frac{1}{2}} T_{\rm e}^{\frac{1}{2}} \,{\rm cm\,s^{-1}}. \tag{19}$$

McWhirter *et al.* (1975) give a convenient form for the conduction damping of sound waves, which they show is more important for the solar transition region and corona than is viscous damping. The damping length is

$$L_{\rm s} = 96.3\, P_{\rm e}\, T_{\rm e}^{-2} (2\pi/\omega)^2, \tag{20}$$

where ω is the frequency of the wave. ($\omega = 2\pi/\tau$ where τ is the wave period.)

Adam (1974) gives a convenient form (derived from Kahalas 1960) for the damping length for the viscous damping of Alfvén waves which reduces to

$$L_{\rm A} = 2.9\times 10^{25} (B_0^3/\omega^2)\, P_{\rm e}^{-\frac{1}{2}}\, T_{\rm e}^{-2}. \tag{21}$$

For the range of conditions in the transition region and inner corona $L_{\rm A}$ and $L_{\rm s}$ are greater than the thickness of the layers considered and the energy dissipated can be given as

$$R_{\rm diss} \simeq \phi/L. \tag{22}$$

As $T_{\rm e} \to T_{\rm c}$, $L \approx \Delta h$ and equation (22) becomes only approximate. Thus the energy deposited by either sound or Alfvén waves is

$$\Delta F_{\rm m}({\rm sound}) = \int_R R_{\rm s\text{-}diss}\, {\rm d}h = 4.0\times 10^{-24} \int_R V^2 \omega^2 T_{\rm e}^{\frac{3}{2}}\, {\rm d}h \tag{23}$$

$$\Delta F_{\rm m}({\rm Alfvén}) = \int_R R_{\rm A\text{-}diss}\, {\rm d}h = 7.0\times 10^{-39} \int_R V^2 (\omega^2/B_0^2)\, P_{\rm e}\, T_{\rm e}^{\frac{3}{2}}\, {\rm d}h. \tag{24}$$

These expressions can now be compared with equations (13) and (14) for the 'observed' distribution of $\Delta F_{\rm m}$.

McWhirter *et al.* (1975) have made a model of the quiet solar atmosphere by deriving a density and temperature distribution as a function of height which is consistent with the energy balance between the conduction damping of sound waves, radiative losses and thermal conduction. However, this model gives an emission measure distribution which is significantly different from that observed. If the values of V and ω by McWhirter *et al.* are substituted in equation (23) then the difference between this expression and that required to fit the 'observed' $\Delta F_{\rm m}$ becomes clear. These values are

$$V^2 = 2\langle V_{\rm m}^2\rangle = 2V_{\rm s}^2, \quad \text{and} \quad \omega = 0.02 = \text{const.}$$

Hence from equation (23),

$$\Delta F_{\rm m}({\rm sound}) = 7.2\times 10^{-19} \int_R T_{\rm e}^{\frac{5}{2}}\, {\rm d}h, \tag{25}$$

which can be compared with

$$\Delta F_{\rm m} = 4.8\times 10^{-17} \int_R P_{\rm e}^2 (1/T_{\rm e}^3)\, {\rm d}h + 3.1\times 10^{-10} T_{\rm e}^{\frac{5}{2}}, \tag{26}$$

where the expression for ${\rm d}T/{\rm d}h$ which fits the observed emission measure has been used in deriving the second (conduction) term. If this expression, i.e. ${\rm d}h/{\rm d}T = adT_{\rm e}^{\frac{5}{2}} P_{\rm e}^{-2}$, is used in both equations (25) and (26), to give

$$\Delta F_{\rm m}({\rm sound}) = 9.45\times 10^{-19} ad P_{\rm e}^{-2}\, T^6$$

PHILOSOPHICAL TRANSACTIONS OF THE ROYAL SOCIETY A MATHEMATICAL, PHYSICAL & ENGINEERING SCIENCES

and $$\Delta F_{\mathrm{m}} = 5.1 \times 10^{-17} a T_{\mathrm{e}}^{\frac{1}{2}} + 3.1 \times 10^{-10} T_{\mathrm{e}}^{\frac{5}{2}}$$

it can be seen that with $P_{\mathrm{e}} \simeq$ constant the temperature dependence for the conduction damping of sound waves with $V = \sqrt{2} V_{\mathrm{s}}$ and ω a constant cannot fit the form of ΔF_{m} required by the observed emission measure. Moreover the absolute value of ΔF_{m} as calculated from equation (23) for the quiet Sun parameters given in § 4 is at least an order of magnitude too small.

Table 4 gives the values of the wave period ($\tau = 2\pi/\omega$) that are obtained using the 'observed' damping lengths and assuming that the dissipation is (*a*) conduction damping of sound waves ($L_0 = L_{\mathrm{s}}$) and (*b*) viscous damping of Alfvén waves ($L_0 = L_{\mathrm{A}}$). For the quiet Sun it can be seen that the wave periods are much shorter than 300 s in the transition region, and that for $B_0 = 1$ G (10^{-4} T) there is little difference between the two sets of results. The peak amplitude velocity is almost constant at *ca.* 30–50 km s^{-1}, i.e. $\langle V_{\mathrm{m}}^2 \rangle^{\frac{1}{2}} \simeq$ 20–35 km s^{-1}, close to the observed values of *ca.* 26–40 km s^{-1} (see later in this section). If L_0 is used directly without assuming a damping mechanism, but with (*a*) $V_{\mathrm{p}} = V_{\mathrm{s}}$, and then (*b*) $V_{\mathrm{p}} = V_{\mathrm{A}}$, it can be seen that the resulting peak amplitude velocities are very similar to those obtained using L_{A} or L_{s}. For the quiet Sun it can be concluded that $V \sim$ 30–50 km s^{-1}, that either conduction damping of sound waves and/or viscous

TABLE 4. EMPIRICAL DAMPING LENGTHS, WAVE FREQUENCY AND PEAK AMPLITUDE VELOCITIES FOR MODELS 1 AND 5

model 1. Quiet Sun, $T = 1.78 \times 10^6$ K

		if $L_0 = L_{\mathrm{s}}$		if $L_0 = L_{\mathrm{A}}$ and $B = 1$ G (10^{-4} T)		using L_0 directly and $V_{\mathrm{p}} = V_{\mathrm{s}}$	using L_0 directly and $V_{\mathrm{p}} = V_{\mathrm{A}}$, $B = 1$ G	observed
lg T / K	L_0 / 10^4 km	τ / s	V / km s^{-1}	τ / s	V / km s^{-1}	V / km s^{-1}	V / km s^{-1}	$\langle V_{\mathrm{m}}^2 \rangle^{\frac{1}{2}}$ ($\simeq 0.71 V_{\mathrm{p}}$) / km s^{-1}
5.3	0.26	16	28	19	38	33	40	26
5.4	0.45	26	33	34	43	38	45	
5.6	0.63	39	33	48	43	38	45	
5.7	1.0	62	36	80	48	42	50	
5.8	1.3	88	36	115	48	42	50	mean 25–40
5.9	2.0	141	43	181	56	49	58	
6.0	2.0	183	38	215	48	43	50	
6.1	3.2	302	43	320	50	46	53	
6.2	5.4	556	44	449	40	44	47	34
6.25								→ 0

model 5. $T_{\max} = 2 \times 10^6$ K

		if $L_0 = L_{\mathrm{s}}$		if $L_0 = L_{\mathrm{A}}$ and $B_0 = 1$ G		using L_0 directly and $V_{\mathrm{p}} = V_{\mathrm{s}}$	using L_0 directly and $V_{\mathrm{p}} = V_{\mathrm{A}}$, $B_0 = 1$ G
lg T / K	L_0 / km	τ / s	V / km s^{-1}	τ / s	V / km s^{-1}	V / km s^{-1}	V / km s^{-1}
5.3	1.6×10^2	0.77	24	12	75	32	98
5.4	3.0×10^2	1.3	25	20	75	34	105
5.5	5.7×10^2	2.2	25	35	75	34	105
5.6	1.0×10^3	3.6	25	59	75	34	105
5.7	2.1×10^3	6.7	27	107	83	37	122
5.8	3.8×10^3	11	28	181	86	36	111
5.9	6.0×10^3	18	26	283	79	35	107
6.0	1.1×10^4	32	27	486	81	36	109
6.1	1.7×10^4	50	25	732	74	34	101
6.2	1.9×10^4	73	23	954	67	31	89
6.3							

PHILOSOPHICAL TRANSACTIONS OF THE ROYAL SOCIETY A MATHEMATICAL, PHYSICAL & ENGINEERING SCIENCES

damping of Alfvén waves could be operating, but that the period of the waves damped in the transition region needs to be 18 s rather than 300 s as observed from chromospheric intensity variations. For the damping and propagation of Alfvén waves the velocities are proportional to $\sqrt{B_0}$, and for $B_0 > 10^{-4}$ T the resulting velocities are smaller than the observed values of $\langle V_m^2 \rangle^{\frac{1}{2}}$.

For active regions the results for the sound velocity case can be regarded as limiting values since in the flux tubes the waves will amost certainly have a magnetic component. For conduction damping of acoustic waves the periods would have to be extremely short – for model 5, less than 1 s at $T_e = 2 \times 10^5$ K. For viscous damping of Alfvén waves and $B_0 \simeq 10^{-4}$ T, the periods are similar to those in the quiet Sun case at $T_e \simeq 2 \times 10^5$ K but become very long, *ca.* 1000 s, at 2×10^6 K. For $B_0 = 10^{-4}$ T, the velocities just become supersonic at the low end of the temperature range. Further work is needed to establish the likelihood of waves with $\tau \lesssim 1$ existing at $T_e \sim 2 \times 10^5$ K, but it should be noted that these short periods are close to the relaxation times for various plasma processes. The very short periods obtained may independently rule out the process of conduction damping of acoustic waves. The periods and velocities for models 2 and 4 are similar or intermediate to those given in table 4.

Similar results are obtained for the velocities if the 'observed' damping lengths are used directly without involving a damping mechanism. For the quiet Sun the values of $V \times 0.71$ are close to the observed values of $\langle V_m^2 \rangle^{\frac{1}{2}}$, whether the propagation velocity is taken as the sound velocity or the Alfvén velocity (and $B_0 = 10^{-4}$ T). For higher fields the velocities become lower than those observed. For a wave travelling at V_A a field of $B_0 = 10^{-4}$ T gives supersonic velocities for V at 2×10^5 K, but only small fields are required to reduce these to below the sound velocity. Other types of waves will have velocities given by $V_p = (V_A^2 + V_s^2)^{\frac{1}{2}}$, so the cases discussed can be used to give limiting values of V_m.

It is difficult to deduce other than limits to the magnetic field in the transition region at $T_e \sim 10^5$ K. For the quiet corona the average field is usually considered to be about 10^{-4} T. If the field is scaled by the area factor corresponding to the supergranulation boundaries a field of about 3×10^{-4} T at $T_e = 2 \times 10^5$ K would be expected. If the field originates from small areas within the boundaries then this is only a lower limit. For the active region loop systems analysed by Gabriel & Jordan (1975) the minimum fields required to at least balance the gas pressure are about $2\text{–}5 \times 10^{-4}$ T (for models 2–5 respectively at $h = 3 \times 10^4$ km). The change in cross-section area of the loops at lower heights is not yet determined and hence the scaling factor for the field at $T_e = 2 \times 10^5$ K is not known.

The observed values for the non-thermal velocities in the temperature region $\sim 10^5$ to 2×10^6 K, given in table 4, have been taken from the following sources. Boland *et al.* (1975) find $\langle V_m^2 \rangle^{\frac{1}{2}} = 26$ km/s at $T_e = 10^5$ K ($\simeq 0.56 V_s$). Similar values for ions formed around $T_e = 10^5 - 2 \times 10^5$ K have been observed by Brueckner & Moe (1973). These authors also measured the width of the Fe XII forbidden line formed at $T_e = 1.7 \times 10^6$ K, and found the line width fitted the normal thermal velocity without any additional non-thermal component. Billings (1966) has also shown in the inner corona where visible region observations are made any non-thermal component to the line width has to be very much less than the thermal component. Feldman & Behring (1974) have obtained widths for e.u.v. lines from ions of O, Mg, Si and S formed in the transition region and inner corona and find velocities in the range 24–40 km/s. Their most reliable measurements for lines of Fe X and Fe XI give $\langle V_m^2 \rangle^{\frac{1}{2}} = 34$ km/s. The lines of He II, for which $T_e \gtrsim 10^5$ K, give rather higher values of $\langle V_m^2 \rangle^{\frac{1}{2}} \simeq 50$ km/s. Overall the observations suggest that $\langle V_m^2 \rangle^{\frac{1}{2}}$ continues at about 30 km/s before finally decreasing in the corona.

PHILOSOPHICAL TRANSACTIONS OF THE ROYAL SOCIETY A MATHEMATICAL, PHYSICAL & ENGINEERING SCIENCES

6. Conclusions

The observed emission measure distribution in quiet and active regions suggests that a general relationship between the emission measure and temperature may be applicable to regions where solar wind losses can be neglected. This general relation can be used together with the equation of hydrostatic equilibrium and the equation of conductive flux to derive simple relations between the following quantities: P_0, the electron pressure in the transition region at T_0; T_c, the temperature of the corona or isothermal component of a flux tube; $F_m(P_0)$, the energy conducted back at T_0, and the total radiation loss above T_0. These relations simplify the calculation of models of both quiet and active regions as a function of chosen parameters. Such models show that the observed properties of flux tubes can be fitted with a range of relative values of the radiative loss term and the conductive flux term.

For the quiet Sun the energy conducted back at $T_e \simeq 2 \times 10^5$ K is balanced by the energy dissipation at close to coronal temperatures as assumed by many authors. However, in the present analysis, which uses a 3/2 power law for the emission measure distribution, some dissipation is needed in the transition region to balance the radiative losses and conductive flux losses which are comparable in magnitude.

In the active region loops the dissipation becomes relatively more important in the transition region and has to balance radiative losses which are substantially larger than the conductive flux losses.

The rate of decrease of the energy F_m with height can be used to derive empirical damping lengths. These can be combined with, for example, the theoretical damping lengths for conduction damping of acoustic waves or for the viscous damping of Alfvén waves, to derive the wave frequency. The energy equation then allows V to be calculated also. For the quiet Sun it is not possible to rule out either damping mechanism on the basis of the velocities derived since they are close to observed values. However, the period of the wave damped would have to vary between 16 s at $T_e = 2 \times 10^5$ K and 550 s in the corona. In the active region loops, however, conduction damping of acoustic waves seems unlikely in view of the extremely short periods $\lesssim 1$ s required. Alternatively the empirical damping lengths can be combined with the energy equation to deduce the peak amplitude velocity, V, for acoustic type waves, or the product $V\sqrt{B}$ for Alfvén type waves, without involving a particular damping mechanism.

For the quiet Sun this approach makes very little difference to the resulting velocities. For the active region loops, however, the velocities become supersonic at $T_e = 2 \times 10^5$ K if $V_p = V_A$. However, only small fields (*ca.* 2×10^{-4} T) are required to give subsonic values of V.

The analysis discussed above should at least provide simple methods by which the overall energy balance in an active region at $T_e > 2 \times 10^5$ K can be studied. Clearly observations with sufficient spatial resolution to resolve sets of loop systems will continue to be required. Further work on the structure of the regions between $T_e \approx 10^4$ and 2×10^5 K is required to link the energy balance to the chromospheric levels. It would, however, be interesting to correlate photospheric field measurements as a function of position in an active region with deduced values of $F_m(P_0)$.

It is a pleasure to acknowledge useful discussions with J. Adam and R. G. Evans.

PHILOSOPHICAL TRANSACTIONS OF THE ROYAL SOCIETY A MATHEMATICAL, PHYSICAL & ENGINEERING SCIENCES

References (Jordan)

Adam, J. 1974 Ph.D. Thesis, University of London.
Athay, R. G. 1966 *Astrophys. J.* **145**, 784.
Billings, D. E. 1966 *A guide to the solar corona.* New York: Academic Press.
Boardman, W. J. & Billings, D. E. 1969 *Astrophys. J.* **156**, 731.
Boland, B. C., Dyer, E. P., Firth, J. G., Gabriel, A. H., Jones, B. B., Jordan, C., McWhirter, R. W. P., Monk, P. & Turner, R. F. 1975 *Mon. Not. R. astr. Soc.* **171**, 697.
Brueckner, G. E. & Moe, O. K. 1973 *Space Research XII*, p. 1595. Berlin: Akademie-Verlag.
Burton, W. M., Jordan, C., Ridgeley, A. & Wilson, R. 1971 *Phil. Trans. R. Soc. Lond.* A **270**, 81.
Culhane, J. L. & Acton, L. W. 1974 *A. Rev. Astron. Astrophys.* **12**, 359.
Dupree, A. K. 1972 *Astrophys. J.* **178**, 527.
Dupree, A. K., Huber, M. C. E., Noyes, R. W., Parkinson, W. H., Reeves, E. M. & Withbroe, G. L. 1973 *Astrophys. J.* **182**, 321.
Feldman, U. & Behring, W. E. 1974 *Astrophys. J.* **189**, L45.
Gabriel, A. H. & Jordan, C. 1975 *Mon. Not. R. astr. Soc.* **173**, 397.
Jordan, C. 1975 IAU Symposium 68 (ed. Kane) 109.
Jordan, C. & Wilson, R. 1971 In *Physics of the solar corona* (ed. Macris), p. 219. Dordrecht, Holland: D. Reidel Publ. Co.
Kahalas, S. L. 1960 *Phys Fluids* **3**, 372.
Kopp, R. A. 1972 *Solar Phys.* **27**, 373.
Kopp, R. A. & Kuperus, M. 1968 *Solar Phys.* **4**, 212.
Krieger, A. S., Vaiana, G. S. & Van Speybroeck, L. P. 1971 In *Solar magnetic fields.* Proc. IAU Symposium No. 43, p. 397.
McWhirter, R. W. P., Thonemann, P. C. & Wilson, R. 1975 *Astron. & Astrophys.* **40**, 63.
Malinovsky, M. & Heroux, L. 1973 *Astrophys. J.* **181**, 1009.
Mason, H. 1975 *Mon. Not. R. astr. Soc.* **171**, 119.
Moore, R. L. & Fung, P. C. 1972 *Solar Phys.* **23**, 79.
Noyes, R. W. 1971 In *Physics of the solar corona* (ed. Macris), p. 192. Dordrecht, Holland: D. Reidel Publ. Co.
Noyes, R. W., Withbroe, G. L. & Kirshner, R. P. 1970 *Solar Phys.* **11**, 388.
Pneuman, G. W. 1972 *Astrophys. J.* **172**, 793.
Reeves, E. M., Foukal, P. V., Huber, M. C. E., Noyes, R. W., Schmahl, E. J., Timothy, J. G., Vernazza, J. E. & Withbroe, G. L. 1974 *Astrophys. J.* **188**, L27.
Shmeleva, O. P. & Syrovatskii, S. I. 1973 *Solar Phys.* **33**, 341.
Tousey, R., Bartoe, J. D., Bohlin, J. D., Brueckner, G. E., Purcell, J. D., Scherrer, V. E., Schumacher, R. J., Sheeley, M. R. & Van Hoosier, M. E. 1973 *Solar Phys.* **33**, 265.
Vaiana, G. S., Krieger, A. S. & Timothy, A. F. 1973 *Solar Phys.* **32**, 81.
Walker, A. B. C. 1975 IAU Symposium 68 (ed. Kane) 73.
Withbroe, G. L. 1970 *Solar Phys.* **11**, 42.

PHILOSOPHICAL TRANSACTIONS OF THE ROYAL SOCIETY A MATHEMATICAL, PHYSICAL & ENGINEERING SCIENCES